Power-Law Solvation Dynamics in G-quadruplex DNA: Role of Hydration Dynamics on Ligand Solvation inside DNA

ARTICLE *in* JOURNAL OF PHYSICAL CHEMISTRY LETTERS · APRIL 2015

Impact Factor: 7.46 · DOI: 10.1021/acs.jpclett.5b00653

5 AUTHORS, INCLUDING:

Him Shweta
Jawaharlal Nehru University
2 PUBLICATIONS **11** CITATIONS
SEE PROFILE

Sachin Dev Verma
University of South Carolina
9 PUBLICATIONS **77** CITATIONS
SEE PROFILE

Sobhan Sen
Jawaharlal Nehru University
36 PUBLICATIONS **1,004** CITATIONS
SEE PROFILE

THE JOURNAL OF PHYSICAL CHEMISTRY Letters

Letter

pubs.acs.org/JPCL

Power-Law Solvation Dynamics in G-Quadruplex DNA: Role of Hydration Dynamics on Ligand Solvation inside DNA

Nibedita Pal,[‡] Him Shweta,[‡] Moirangthem Kiran Singh, Sachin Dev Verma, and Sobhan Sen*

Spectroscopy Laboratory, School of Physical Sciences, Jawaharlal Nehru University, New Delhi 110067, India

Supporting Information

ABSTRACT: G-quadruplex DNA (GqDNA) structures act as promising anticancer targets for small-molecules (ligands). Solvation dynamics of a ligand (DAPI: 4′,6-diamidino-2-phenylindole) inside antiparallel-GqDNA is studied through direct comparison of time-resolved experiments to molecular dynamics (MD) simulation. Dynamic Stokes shifts of DAPI in GqDNA prepared in H_2O buffer and D_2O are compared to find the effect of water on ligand solvation. Experimental dynamics (in H_2O) is then directly compared with the dynamics computed from 65 ns simulation on the same DAPI-GqDNA complex. Ligand solvation follows power-law relaxation (summed with fast exponential relaxation) from ∼100 fs to 10 ns. Simulation results show relaxation below ∼5 ps is dominated by water motion, while both water and DNA contribute comparably to dictate long-time power-law dynamics. Ion contribution is, however, found to be negligible. Simulation results also suggest that anomalous solvation dynamics may have origin in subdiffusive motion of perturbed water near GqDNA.

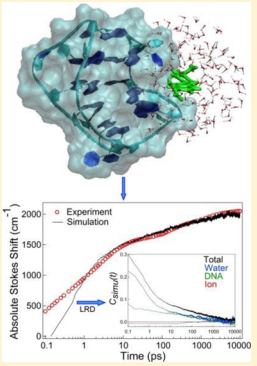

The fact that water does not act as mere spectator-solvent for biomolecules but maintains structure and function of biomolecules is well established.[1] Dynamics of water in-and-around biomolecules facilitate important biochemical processes ranging from enzyme catalysis,[2] protein folding,[3] to interaction of DNA with proteins[4] and drugs (ligands).[5] In fact, this letter will show that dynamics of water is crucial for ligand solvation inside DNA (i.e., G-quadruplex DNA).

Of recent interest, G-quadruplex DNA (GqDNA) structures attracted tremendous attention because of their therapeutic role in cancer treatment.[6,7] These structures are formed by self-assembly of repetitive guanine-rich DNA sequence in the presence of Na^+ or K^+ ions and/or small molecules (ligands), stabilized by Hoogsteen-type hydrogen bonds between guanines.[8−14] The fact that these structures are not only formed in vitro[6−11] but also in human cells[12] has sparked huge activities to develop ligands that can target GqDNA for efficient antitumor effects.[13,14] Unlike Watson−Crick duplex-DNA, GqDNA has high structural diversity. It has been found that change in local hydration/solvation state drastically induces structural polymorphism in GqDNA,[15,16] thereby strongly affecting ligand binding to these structures;[17] however, despite the availability of large sum of structural data,[6,8,13−16] it is still unknown how dynamics of water and ions solvate ligand inside GqDNA.

This letter tackles these issues by measuring dynamic Stokes shift of a ligand (DAPI: 4′,6-diamidino-2-phenylindole) in antiparallel-GqDNA prepared in H_2O buffer and D_2O and comparing the Stokes shift dynamics (in H_2O) directly to the dynamics computed from 65 ns molecular dynamics (MD) simulation. We show dynamics of ligand solvation in GqDNA follow power-law relaxation (summed with fast exponential relaxation) from ∼100 fs to 10 ns, similar as previously observed in duplex-DNA.[26,27] Simulation results show water (and DNA-proper) controls the dynamics but with negligible contribution from ions. The broad distribution of water residence times and sublinear mean-square displacements (MSDs) of water near the ligand indicate that anomalous solvation dynamics may have origin in the subdiffusive motion of perturbed water near GqDNA.

Time-resolved fluorescence Stokes shift (TRFSS) experiments can measure dynamics on subpicosecond to nanosecond time scales, and hence they have been widely used to study solvation dynamics in water,[18] proteins,[19,20] DNA,[21−31] protein−DNA complexes,[32,33] ionic liquids,[34,35] macromolecular systems,[36] and even biological cells.[37] TRFSS measures collective dynamics of electrostatic interactions of a chromophore probe with its surrounding molecules.[18] Charge distribution in probe changes upon optical excitation. Subsequently, surrounding dipolar/charged molecules move to stabilize their interaction energy with probe. Time-dependent lowering of energy is then captured as probe's fluorescence frequency shift, which in turn measures solvation dynamics of probe's local environment. MD simulations, on the other hand, are shown to have excellent capability to interpret the experimental results.[39−46]

Proteins and DNA are different in many ways, but their underlying dynamical features are found to be similar. Considerable efforts have gone into understanding the dynamics in proteins and DNA through experiments,[19−31] theory,[38] and simulations.[39−55]Dynamics in these biomolecules extend in times >10 ps,[19−31] while in simple water dynamics

Received: March 30, 2015
Accepted: April 23, 2015
Published: April 23, 2015

DOI: 10.1021/acs.jpclett.5b00653
J. Phys. Chem. Lett. 2015, 6, 1754−1760

complete in a few picoseconds.[18] In many occasions, dynamics in proteins and DNA are found to be nonexponential and dispersed and extend in several time decades, showing stretched-exponential[49] or logarithmic[50,51] or even power-law relaxation.[26−29,40,43,51,52] Explanation of such dispersed dynamics remains elusive primarily because of its very origin from intricate coupling between motions of components in biomolecular solution (i.e., water, ions, and biomolecule). The question remains whether the motion of water or ions or biomolecule or the inextricable coupled motions of these components control the dynamics.[19,39−46] Nevertheless, compared with proteins, studies on DNA solvation dynamics are limited, and also the primary focus has been only on duplex DNA.[21−31,38−43]

Here we use 22-mer (5′-AGGG(TTAGGG)$_3$-3′) human telomeric DNA sequence to make antiparallel-GqDNA[8] structure in H_2O buffer and D_2O with 100 mM NaCl and study the solvation dynamics. (See the Supporting Information (SI) for materials and methods.) DAPI is used as probe ligand that binds to antiparallel-GqDNA with binding constant 2.7 × 10^5 M^{-1}. (See the SI.) DAPI binding to GqDNA was not previously studied. Molecular docking, followed by MD simulation, shows DAPI binds to one of the smaller grooves of antiparallel-GqDNA created by G14−G16. (See the SI.) To cover the broad time range of dynamics we combine time-resolved emission spectra (TRES) of DAPI in GqDNA, constructed from decays measured in fluorescence upconversion (UPC; TRES range: 100 fs to 500 ps) and time-correlated single photon counting (TCSPC; TRES range: ∼30 ps to 10 ns). Log-normal fits to TRES are used for calculating time-dependent Stokes shifts in terms of first moment (mean) frequencies. Finally, the "absolute" Stokes shift is calculated by subtracting mean frequencies of TRES from the mean frequency of (time-zero) glass spectra measured at −78 °C, which reports only diffusive solvation dynamics because in glass the diffusive motions are frozen but vibrational and inertial motions can persist. (See the SI.)[26−30]

Figure 1A compares the absolute Stokes shifts of DAPI in GqDNA prepared in H_2O buffer and D_2O from 100 fs to 10 ns. It can be seen that the rate of Stokes shifts in both H_2O and D_2O samples are slow and dispersed, but below ∼5 ps the rate gets faster. Comparison of two data sets also finds that there is subtle difference in the overall Stokes shift rates in H_2O and D_2O. (See Figure S7B in the SI.) The Stokes shifts of DAPI in GqDNA within the measured time window (100 fs to 10 ns) are found to be 1643 cm^{-1} in H_2O and 1567 cm^{-1} in D_2O. The Stokes shifts data of both samples are modeled with power law, summed with exponential relaxation which accommodates fast dynamics below ∼5 ps as[26]

$$S(t) = S_\infty\left[a\left(1 - \left(1 + \frac{t}{t_0}\right)^{-n}\right) + b(1 - e^{-t/\tau})\right] \quad (1)$$

Equation 1 fits data in H_2O with parameters S_∞ = 2370 cm^{-1}, a = 0.9, t_0 = 35 fs, n = 0.16, b = 0.1, and τ = 2 ps. Fit extracts slow dynamics as power-law relaxation of exponent 0.16 and fast dynamics as exponential relaxation of 2 ps. Note that solvation dynamics in pure water occurs in ∼1 ps;[18] however, hydration dynamics near biomolecular surface is found to become retarded by a factor of 2 to 3 compared with pure water.[47] The 2 ps relaxation may arise from interfacial water dynamics near GqDNA. Fit to D_2O data finds ∼1.8 fold slower exponential relaxation of 3.7 ps (with b = 0.08) and more

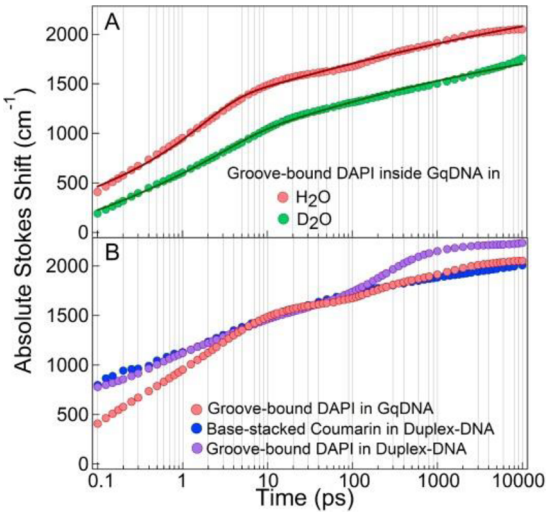

Figure 1. (A) Comparison of absolute Stokes shifts of DAPI in GqDNA prepared in H_2O buffer (pink) and D_2O (green). Lines through points show fits using eq 1. Data show faster relaxation below ∼5 ps and power-law type slow relaxation beyond ∼5 ps until 10 ns. (B) Comparison of "absolute" Stokes shift of DAPI in GqDNA (pink) to previous Stokes shift data of DAPI (purple) and coumarin (blue) in duplex-DNA.[26,27] The duplex-DNA data are shifted vertically to match with GqDNA data. In times >5 ps the power-law dynamics of DAPI in GqDNA is similar to coumarin (blue) in duplex-DNA but different from DAPI (purple) in duplex-DNA. (See the text for details.)

dispersed power-law relaxation of exponent 0.09 (a = 0.92, S_∞ = 2400 cm^{-1}, t_0 = 40 fs) compared with that in H_2O. Retardation in fast relaxation on replacing H_2O with D_2O by a factor of ∼1.4 in duplex-DNA was observed by Ernsting and coworkers.[24] A similar effect is seen here that indicates water controls the fast dynamics. Present data also show power-law dynamics is affected by D_2O as well. These results infer that water contributes substantially to the overall solvation dynamics. This we also confirm from MD simulation results. (See below.)

TRFSS studies with probes placed inside duplex-DNA by either covalent attachment (replacing base/base-pair) or minor groove-binding have been performed.[21−31] Berg et al. were the first to use covalently attached base-stacked probe (coumarin/abasic pair) and show that DNA dynamics extend into nanosecond time scales.[21] Zewail et al. reported TRFSS of base-stacked 2-aminopurine and groove-bound Hoechst until 100 ps to show that both probes sense similar dynamics in duplex-DNA.[22,23] Ernsting et al. reported TRFSS of base-stacked probe (HNF) to show water controls local dynamics inside duplex-DNA.[24] Pal et al. reported nanosecond dynamics in duplex-DNA using groove-bound probes, Hoechst and DAPI.[25] However, combining TRFSS data of coumarin from different techniques, Berg et al. showed that Stokes shift dynamics in duplex-DNA actually follow a power law with exponent 0.15 from 40 fs to 40 ns.[26,27] Recently, some of us have also shown that TRFSS of groove-bound DAPI in duplex-DNA follows a similar power law until ∼100 ps, but beyond this time the dynamics converge rapidly to an equilibrium near 10 ns.[28,29] Nonetheless, it was not known whether power law relaxation is a feature common to other DNA structures.

Figure 1B compares absolute Stokes shifts of DAPI in GqDNA with previous data of base-stacked coumarin and groove-bound DAPI in duplex-DNA.[26,27] Comparison finds that in times >5 ps until 10 ns the power-law dynamics probed

DOI: 10.1021/acs.jpclett.5b00653
J. Phys. Chem. Lett. 2015, 6, 1754−1760

by DAPI in G-rich human telomeric GqDNA is almost identical to the dynamics probed by coumarin in duplex-DNA with generic sequence.[26,27] This result clearly proves the generality of similar power-law solvation dynamics in different DNA structures. Below ~5 ps a distinct fast relaxation appears in GqDNA that is absent in duplex-DNA (Figure 1B). This can arise from loose binding of DAPI in GqDNA (2.7×10^5 M^{-1}) compared with duplex-DNA, which may lead to a situation where DAPI stays more exposed toward water such that both fast and slow motion of (perturbed) water contribute to solvate DAPI in GqDNA. The effect of D_2O on both fast and slow dynamics is an indication of such situation. We confirm these conclusions from MD simulation as discussed later.

Much of the current understanding on DNA solvation dynamics comes from MD simulation studies.[39−43] Hynes, Bagchi, and coworkers in their duplex-DNA simulation found slow dynamics, which they assigned to water and ion motions, but simulation was not long enough to capture nanosecond dynamics.[39] Using 46 ns of simulation, Sen et al. found excellent agreement between TRFSS of coumarin and correlation of simulated electric field in duplex-DNA.[40] This study also found that water controls the power-law dynamics in DNA. However, Furse and Corcelli simulated duplex-DNA with groove-bound Hoechst, similar as in experiment of Zewail, and saw that slow dynamics until 350 ps is dominated by DNA motion but not water or ion motions.[41,42] When they extended their simulation to hundreds of nanoseconds and compared the results to simulated dynamics of coumarin/abasic pair, they saw significant contribution of abasic-site flipping motion to the slow (power-law type) relaxation.[43] These results indicate that despite repeated observation of power-law dynamics in duplex-DNA, explanation of such dynamics remains difficult.[39−43]

To quantify and explain the dispersed solvation dynamics in GqDNA, we performed 65 ns all-atom equilibrium MD simulation on docked DAPI-GqDNA structure in AMBER-12[54] using *parm99* force field, 4940 TIP3P water molecules, and 19 Na^+ ions. Ground-state atomic charges and force field of DAPI were obtained from report of Sponer et al.[55] (See the SI for details.) Molecular docking, followed by MD simulation, shows DAPI binds to one of the smaller grooves of antiparallel GqDNA created near G14−G16. The location of DAPI is found to be constant (within ±0.5 Å) during the entire simulation run, which rules out possibility of diffusive contribution from the probe to the measured dynamics. (See Figure S10D in the SI.)

We calculated electrostatic interaction energy of DAPI with surrounding water, ions, and DNA from MD trajectory using damped shift force (DSF) sum,[56] similar as used previously in simulation of duplex-DNA.[41−43] (See the SI.) The energy of the total system and individual components is plotted in Figure 2A, where water and DNA energies are large, which anticorrelate strongly. (See Figure S11 in the SI.) Ion contribution is, however, found to be insignificant. The total equilibrium solvation correlation function, $C_{simu}(t)$, is then calculated from total energy fluctuations as[39]

$$C_{simu}(t) = \frac{\langle \Delta E(0)\Delta E(t)\rangle_g}{\langle \Delta E(0)^2\rangle_g} \quad (2)$$

where $\Delta E(t) = (E(t) - \langle E(t)\rangle)_g$, is fluctuation in interaction energy of (ground state) DAPI charges and partial charges of surrounding water, ions, and DNA relative to average energy.

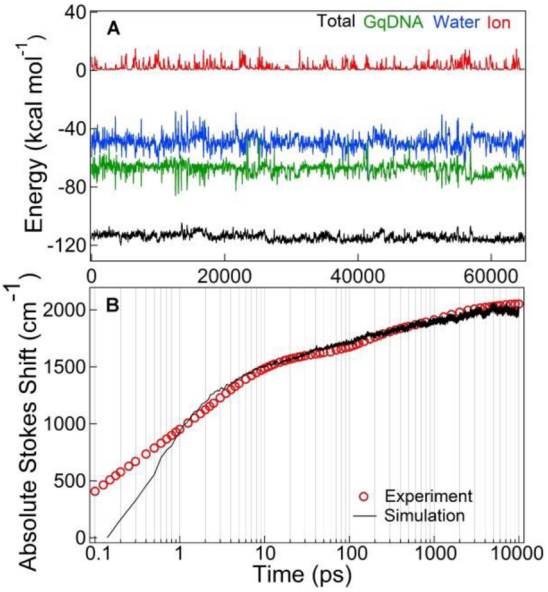

Figure 2. (A) Electrostatic interaction energy of DAPI with ions (red), water (blue), DNA (green), and total system (black) over 65 ns simulation calculated using DSF sum. Energies are calculated at the 0.1 ps step. Energy fluctuations are smoothed with 50 ps running average for clarity in representation. (B) Comparison of "absolute" Stokes shifts of DAPI in GqDNA obtained from experiment and simulation. Limited time resolution of UPC setup (~270 fs) could not allow for extraction of dynamics by ~450 cm^{-1} at 100 fs, which leads to the deviation between experimental and simulation data below ~600 fs. (See the text for details.)

Within linear response approach, solvation correlation functions calculated from (ground-state) equilibrium simulation, $C_{simu}(t)$, and nonequilibrium experiment, $C_{expt}(t)$, can be directly compared;[39,40] however, comparison is not straightforward because $C_{simu}(t)$ includes a large part (~60−80%) of fast inertial component, which is absent in experimental Stokes shifts. We compare simulated and experimental results directly by calculating (simulated) absolute Stokes shift from (simulated) correlation function as[40]

$$S(t) = \delta S_0 + s[1 - C_{simu}(t)] \quad (3)$$

Here δS_0 is the inertial part and s is the total (simulated) Stokes shift. Figure 2B shows the comparison of two data (in H_2O) from 100 fs to 10 ns. Matching is extremely good beyond ~600 fs. Matching require $\delta S_0 = -5338$ cm^{-1} and $s = 7400$ cm^{-1}, which indicate that ~72% of inertial contribution (δS_0) is subtracted from total simulated Stokes shift (s). Note here that time resolution of our UPC setup (~270 fs) limits full extraction of dynamics by 450 cm^{-1} at 100 fs. (See Figure 1A.) This leads to the observed deviation between two data below ~600 fs. Nonetheless, the matching (beyond ~600 fs) not only validates linear response theory[57] but also confirms that the starting docked structure of DAPI-GqDNA and simulation methods used are correct. (The reproducibility of simulation data is also checked from another independent simulation run of 50 ns; see the SI for details.) Fitting to simulated correlation finds similar power-law relaxation ($n = 0.14$) but added with two exponential time-constants of 1.8 ps, similar as found in experiment, and 0.45 ps, which remains unresolved in experiment due to limited time resolution (Figure S13 in SI).

To find the origin of power law and exponential dynamics, we decomposed $C_{simu}(t)$ into partial correlations of water, ions,

DOI: 10.1021/acs.jpclett.5b00653
J. Phys. Chem. Lett. 2015, 6, 1754−1760

and DNA using linear response decomposition (LRD) method.[45] In LRD, $C_{simu}(t)$ is expressed as sum of partial correlations of individual components as[41−46]

$$C_{simu}(t) = \sum_i \frac{\langle \Delta E_i(t) \Delta E(0) \rangle}{C(0)} \quad (4)$$

where i is individual component (i.e., water, ions and DNA proper) and $C(0)$ is total correlation at zero time. Figure 3A plots the partial correlations of water, ions, and DNA along with the total correlation. It can be seen that below ∼10 ps water contributes the most, while both water and DNA contribute almost equally to dictate the power-law relaxation in longer times. The strong anticorrelation between water and DNA energy is an indication of such behavior. (See Figure S11 in the SI.) We note here that the signal-to-noise ratios in the decomposed water and DNA correlations beyond ∼1 ns are not satisfactory. Longer simulation (or averaging of many MD runs of similar lengths) is necessary to improve the quality of (decomposed) data beyond ∼1 ns. The total correlation, however, has good signal-to-noise ratio in long times, which compares extremely well with experimental data. (See Figure 2B.) Figure 3A shows that DNA correlation follows nearly a power-law over the entire time range, while relaxation below ∼5 ps is dominated by water dynamics. Results also reveal that dynamic contribution from ion solvation of all 19 Na^+ is negligible over the entire time range. It is found that water contributes ∼65% to the overall dynamics, while DNA contribution comes next, and ions have little or no effect.

To find the range of interactions of water and DNA with ligand we perform spatial decomposition of water shells and DNA parts using LRD. Figure 3B plots the contributions from water within shells of radii 4 Å (first solvation shell), 4−8 Å (second solvation shell), 8−12 Å (third solvation shell), and >12 Å (bulk). It shows fast (exponential) relaxation and long tail of slow dynamics originate from water within 4 Å. Around 62% of total water contribution originates from first-shell water. More importantly, nearly a single power-law relaxation (similar to DNA) originates from water in second shell (∼37% of total water contribution); however, water contributions from the third shell and beyond are negligible. To further separate the contributors of fast and slow dynamics in the first shell, we decomposed first-shell water into *inner* (within 7.6 Å of DNA) and *outer* (beyond 7.6 Å of DNA) water using LRD and plotted in Figure 3C. (See the SI for decomposition criteria.) Figure 3C suggests that fast and slow relaxations can be approximately assigned to *outer* and *inner* water molecules, respectively. The subdivision of first-shell water finds ∼9 *inner* and ∼28 *outer* water molecules on average come near DAPI over the entire simulation run. (See Figure 3E.) We also calculated the effective range of DNA contribution, which shows DNA parts within ∼9 Å of DAPI, consisting of A13−T17 and G20−G22, dictate the DNA correlation (Figure 3D). A cartoon highlighting parts of water and DNA that control the total dynamics is presented in Figure 3E.

The explanation of dispersed solvation dynamics in biomolecules remains difficult. Various theoretical approaches have been adopted to explain the anomalous dynamics in biomolecules.[38,47−51,58−62,64] It has been found that anomalous hydration dynamics near biomolecules can be traced back to the sublinear diffusion of water on fractal biomolecular surface or rugged potential energy landscape created by the biomolecule.[48,51] Other approaches such as mode-coupling

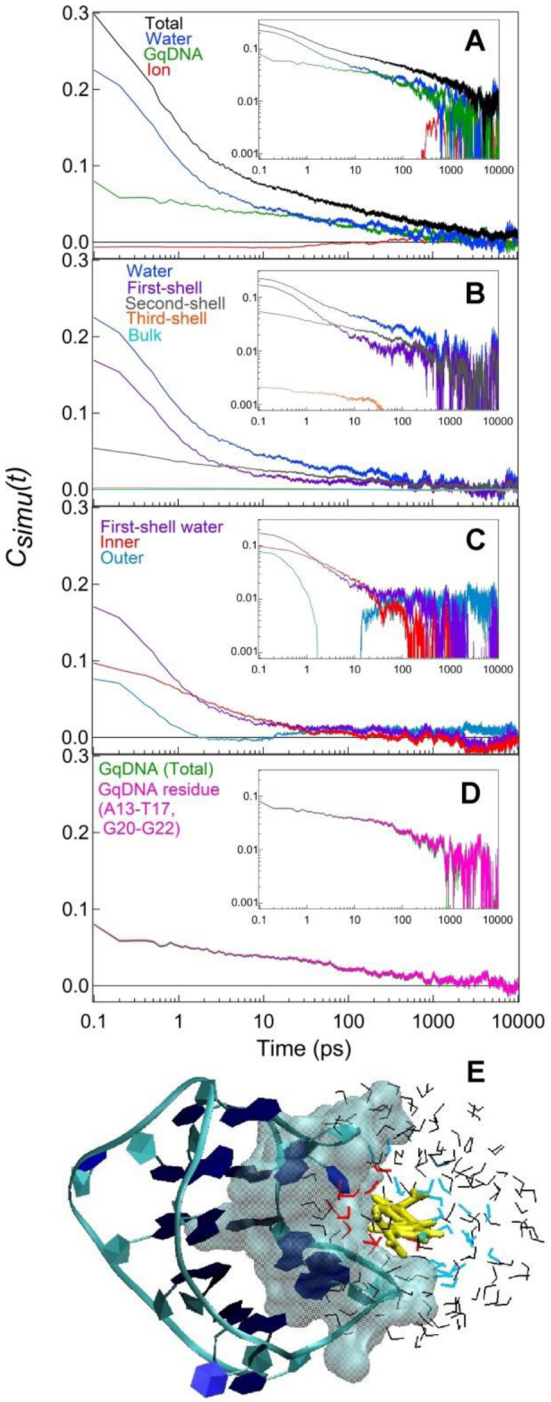

Figure 3. (A) Linear response decomposition (LRD) of total simulated correlation (black) into water (blue), DNA (green), and ion (red) correlations. (B) Spatial decomposition of water into first (within 4 Å), second (within 4−8 Å), third (within 8−12 Å) solvation shells, and bulk (>8 Å) around DAPI. Power-law-type relaxation originates from second-shell water, while the fast relaxation together with the long tail of slow dynamics originates from first-shell water. (C) Spatial decomposition of first-shell water into *inner* (within 7.5 Å of DNA) and *outer* (beyond 7.5 Å of DNA) water that approximately separate the fast and slow relaxations of first-shell water-correlation, respectively. (D) Correlation from DNA parts (A13−T17 and G20−G22) that defines the DNA correlation. (E) Simulation snapshot showing water molecules in first solvation shell (red: *inner* and cyan: *outer* water) and second solvation shell (black) around DAPI. The part of DNA that defines DNA correlation is shown as molecular surface. It

DOI: 10.1021/acs.jpclett.5b00653
J. Phys. Chem. Lett. 2015, 6, 1754−1760

Figure 3. continued

is found that materials (water and DNA parts) within ~9 Å of DAPI control the total dynamics in GqDNA. (See the text for details.)

theory (MCT)[38] and molecular jump water reorientation model[47,64] have also been proposed. Water motion on rugged potential surface can lead to a situation where water residence-time distribution shows power-law tail, indicating broad distribution of water trapping times in local minima across the rugged potential surface.[48,51] In such cases, the MSDs of water near biomolecule show sublinear diffusion as $\langle \Delta r(t)^2 \rangle \approx At^{\alpha}$ with $\alpha < 1$.[48,49,59−62] We calculated residence times of first and second shell water, where all 4940 water molecules visit the first and second shells some time or the other within the entire simulation run (Figure 4A,B). There are several water molecules having residence times >1 ns in the first shell, and many having residence time >100 ps in the second shell (Figures 4A,B). At least four hydration sites near the DAPI-GqDNA interface are also found that occupy with water of residence times >3 ns. (See Figure S10C in the SI.) The distributions of residence times for first- and second-shell waters are plotted in Figure 4C, which clearly show power-law behavior in long times. This may indicate that motion of hydration water is perturbed by DNA in such a manner that it creates broad distribution of activation barriers for water exchange between different sites, which may lead to broad distribution of solvent relaxation times. To check the sublinear (translational) diffusion of water we picked those first-shell waters that have residence times >1 ns and calculated their (time-averaged) MSD. The diffusion shows sublinear behavior with MSD following $\sim t^{0.91}$ (Figure 4D). The small deviation from normal diffusion ($\alpha = 1$) may suggest that most of first-shell waters are mobile such that they control fast exponential relaxation (of ~2 ps), while few others contribute to the slow tail of dynamics. In fact, we found that a subset of first-shell water follows MSD of $\sim t^{0.43}$ (Figure 4D), suggesting weak ergodicity breaking in the system.[63] This can explain the origin of the long tail of slow dynamics in first-shell water correlation. (See Figure 3B.) Population splitting of diffusing particles has been treated in theoretical modeling of biomolecular systems.[59−63] Using aging renewal theory it has been shown that in nonstationary processes time aging can actually induce population splitting of diffusing particles with different mobility.[62,63] Such aging effect on subdiffusive motion of water at lipid membrane surface has been found.[65] A similar situation seems to hold in the present GqDNA system. The second-shell water molecules, with residence times >110 ps, show a highly sublinear behavior of MSD following $\sim t^{0.49}$ (Figure 4E). On the basis of these results, we conclude that water with broad distribution of residence times may have different trapping times on the rugged potential surface, which may lead to the observed power-law solvation dynamics in GqDNA.

The field of G-quadruplex DNA research is growing fast, and with new quadruplex structures and ligands being found time and again, the possibility of targeting these DNA structures with ligands for efficient cancer therapy is becoming higher; however, effective drug targeting to any DNA structure requires detailed understanding of local solvation around drugs inside DNA. This letter attempted such a study in GqDNA through direct comparison of experiments to simulation. Results show hydration dynamics is crucial for ligand solvation inside

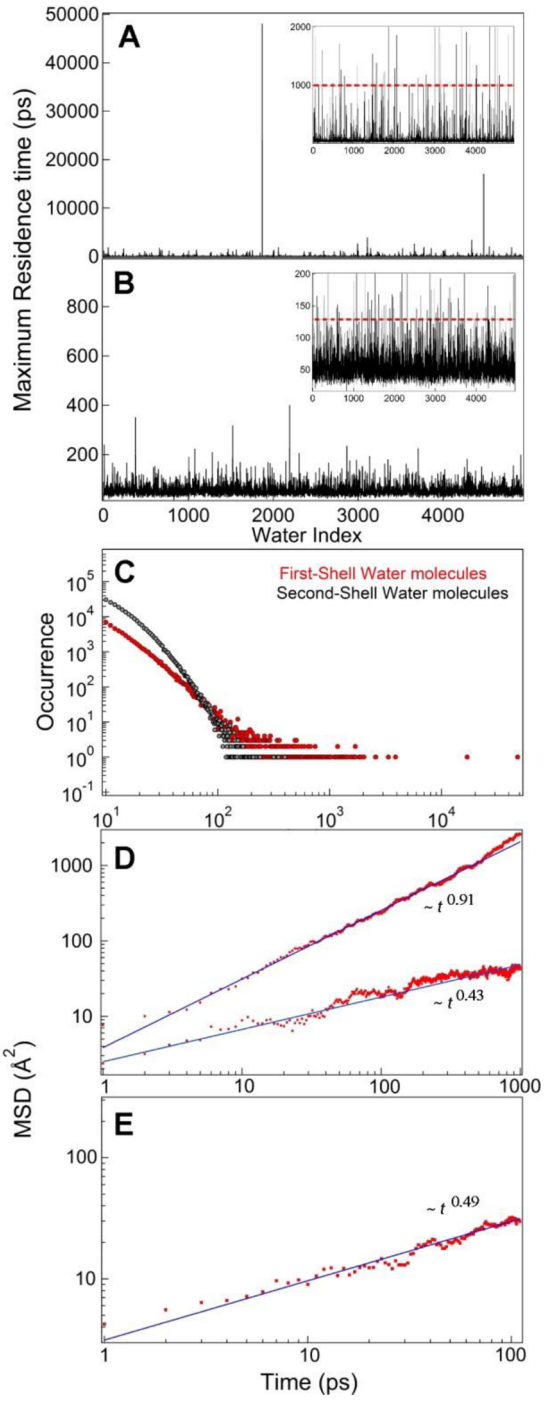

Figure 4. Maximum residence times of all 4940 water molecules that visit first solvation shell (A) and second solvation shell (B). The red dotted lines in insets show the lower limit above which the water molecules were considered for mean-square displacement (MSD) calculations. (C) Distribution of residence times of all water molecules in first (red) and second (gray) solvation shells. The tails of distributions show linear dependence with time in log−log plot. Mean-square displacements (MSD) of first-shell (A) and second-shell (B) water molecules, which are chosen based on the residence times >1 ns and >110 ps, respectively. (See insets in panels A and B.) MSD was calculated at the 1 ps step. First-shell water molecules show sublinear diffusion with MSD $\approx t^{0.91}$, while a subset of these water molecules shows MSD $\approx t^{0.43}$. Second-shell water shows sublinear diffusion with MSD $\approx t^{0.49}$.

DOI: 10.1021/acs.jpclett.5b00653
J. Phys. Chem. Lett. 2015, 6, 1754−1760

GqDNA. The dispersed (power-law) solvent relaxation near DNA may have important biological implications in the interactions of charged/dipolar molecules with DNA. The slow hydration around DNA may have a direct role in capturing (charged/dipolar) ligands and other macromolecules from bulk and stabilizing them near/inside DNA-grooves or in-between DNA bases. In fact, the dynamics of water uptake/release is shown to facilitate drug binding to duplex-DNA, a process that occurs on a complex free-energy surface.[5] The dispersed hydration dynamics may have direct role on defining such complex free-energy landscape. Moreover, the exposure of telomeric ends of DNA toward cellular water may have further importance in the functioning of GqDNA, especially in their interactions with drugs. Nevertheless, further studies are necessary to gain complete knowledge on dispersed dynamics in DNA, and combination of experiment and simulation will be extremely useful for such studies in complex biomolecular systems.

■ ASSOCIATED CONTENT

Supporting Information

Detailed experimental and simulation methods, data analysis, additional data, and text. The Supporting Information is available free of charge on the ACS Publications website at DOI: 10.1021/acs.jpclett.5b00653.

■ AUTHOR INFORMATION

Corresponding Author

*E-mail: sens@mail.jnu.ac.in.

Author Contributions

‡N.P. and H.S. contributed equally.

Notes

The authors declare no competing financial interest.

■ ACKNOWLEDGMENTS

This work is supported by Department of Biotechnology (DBT BUILDER), Department of Science and Technology (DST-FIST), and JNU-UPE-II scheme. We thank Dr. D. Choudhury (SBT, JNU) and Dr. Aswani Tripathi (SPS, JNU) for helpful discussion on simulation methods and Dr. Pritam Mukhopadhyay (SPS, JNU) for the use of fluorometer. UPC, TCSPC, and CD data were collected at AIRF, JNU. N.P. and M.K.S. thank CSIR and H.S. and S.D.V. thank UGC for fellowships.

■ DEDICATION

We dedicate this work to Prof. Kankan Bhattacharyya on the occasion of his 60th birthday in recognition of his mentorship and perseverance in the field of solvation dynamics study of complex systems.

■ REFERENCES

(1) Bagchi, B. *Water in Biological and Chemical Processes: From Structure and Dynamics to Function*; Cambridge University Press: Cambridge, U.K., 2013.

(2) Grossman, M.; Born, B.; Heyden, M.; Tworowski, D.; Fields, G. B.; Sagi, I.; Havenith, M. Correlated Structural Kinetics and Retarded Solvent Dynamics at the Metalloprotease Active Site. *Nat. Struct. Mol. Biol.* **2011**, *18*, 1102−1108.

(3) Kim, S. J.; Born, B.; Havenith, M.; Gruebele, M. Real-Time Detection of Protein-Water Dynamics upon Protein Folding by Terahertz Absorption Spectroscopy. *Angew. Chem., Int. Ed.* **2008**, *47*, 6486−6489.

(4) Gorfe, A. A.; Caflisch, A.; Jelesarov, I. The Role of Flexibility and Hydration on the Sequence-Specific DNA Recognition by the Tn916 Integrase Protein: A Molecular Dynamic Analysis. *J. Mol. Recognit.* **2004**, *17*, 120−131.

(5) Mukherjee, A.; Lavery, R.; Bagchi, B.; Hynes, J. T. On the Molecular Mechanism of Drug Intercalation onto DNA: A Simulation Study of the Intercalation Pathway, Free Energy, and DNA Structural Changes. *J. Am. Chem. Soc.* **2008**, *130*, 9747−9755.

(6) Neidle, S. The Structures of Quadruplex Nucleic Acids and their Drug Complexes. *Curr. Opin. Struct. Biol.* **2009**, *19*, 239−250.

(7) Zahler, A. M.; Williamson, J. R.; Cech, T. R.; Prescott, D. M. Inhibition of Telomerase by G-Quartet DNA Structures. *Nature* **1991**, *350*, 718−720.

(8) Wang, Y.; Patel, D. J. Solution Structure of the Human Telomeric Repeat d[AG3(T2AG3)$_3$] G-Tetraplex. *Structure* **1993**, *1*, 263−282.

(9) Balasubramanian, S.; Hurley, L. H.; Neidle, S. Targeting G-Quadruplexes in Gene Promoters: A Novel Anticancer Strategy. *Nat. Rev. Drug Discovery* **2011**, *10*, 261−275.

(10) Verma, S. D.; Pal, N.; Singh, M. K.; Shweta, H.; Khan, M. F.; Sen, S. Understanding Ligand Interaction with Different Structures of G-Quadruplex DNA: Evidence of Kinetically Controlled Ligand Binding and Binding-Mode Assisted Quadruplex Structure Alteration. *Anal. Chem.* **2012**, *84*, 7218−7226.

(11) Agarwal, T.; Roy, S.; Kumar, S.; Chakraborty, T. K.; Maiti, S. In the Sense of Transcription Regulation by G-Quadruplexes: Asymmetric Effects in Sense and Antisense Strands. *Biochemistry* **2014**, *53*, 3711−3718.

(12) Biffi, G.; Tannahill, D.; McCafferty, J.; Balasubramanian, S. Quantitative Visualization of DNA G-Quadruplex Structures in Human Cells. *Nat. Chem.* **2013**, *5*, 182−186.

(13) Jain, A. K.; Bhattacharya, S. Interaction of G-Quadruplexes with Nonintercalating Duplex-DNA Minor Groove Binding Ligands. *Bioconjugate Chem.* **2011**, *22*, 2355−2368.

(14) Monchaud, D.; Teulade-Fichou, M. P. A Hitchhiker's Guide to G-quadruplex Ligands. *Org. Biomol. Chem.* **2008**, *6*, 627−636.

(15) Miller, M. C.; Buscaglia, R.; Chaires, J. B.; Lane, A. N.; Trent, J. O. Hydration is a Major Determinant of the G-Quadruplex Stability and Conformation of the Human Telomere 3′ Sequence of d(AG3(TTAG3)$_3$. *J. Am. Chem. Soc.* **2010**, *132*, 17105−17107.

(16) Heddi, B.; Phan, A. T. Structure of Human Telomeric DNA in Crowded Solution. *J. Am. Chem. Soc.* **2011**, *133*, 9824−9833.

(17) Chen, Z.; Zheng, K.; Hao, Y.; Tan, Z. Reduced or Diminished Stabilization of the Telomere G-Quadruplex and Inhibition of Telomerase by Small Chemical Ligands under Molecular Crowding Condition. *J. Am. Chem. Soc.* **2009**, *131*, 10430−10438.

(18) Jimenez, R.; Fleming, G. R.; Kumar, P. V.; Maroncelli, M. Femtosecond Solvation Dynamics of Water. *Nature* **1994**, *369*, 471−473.

(19) Li, T.; Hassanali, A. A.; Kao, Y.-T.; Zhong, D.; Singer, S. J. Hydration Dynamics and Time Scales of Coupled Water-Protein Fluctuations. *J. Am. Chem. Soc.* **2007**, *129*, 3376−3382.

(20) Chang, C.-W.; He, T.-F.; Guo, L.; Stevens, J. A.; Li, T.; Wang, L.; Zhong, D. Mapping Solvation Dynamics at the Function Site of Flavodoxin in Three Redox States. *J. Am. Chem. Soc.* **2010**, *132*, 12741−12747.

(21) Brauns, E. B.; Madaras, M. L.; Coleman, R. S.; Murphy, C. J.; Berg, M. A. Measurement of Local DNA DNA Reorganization on the Picosecond and Nanosecond Time Scales. *J. Am. Chem. Soc.* **1999**, *121*, 11644−11649.

(22) Pal, S. K.; Zhao, L.; Zewail, A. H. Water at DNA Surfaces: Ultrafast Dynamics in Minor Groove Recognition. *Proc. Natl. Acad. Sci. U.S.A.* **2003**, *100*, 8113−8118.

(23) Pal, S. K.; Zhao, L.; Xia, T.; Zewail, A. H. Site- and Sequence-Selective Ultrafast Hydration of DNA. *Proc. Natl. Acad. Sci. U.S.A.* **2003**, *100*, 13746−13751.

(24) Dallmann, A.; Pfaffe, M.; Mügge, C.; Mahrwald, R.; Kovalenko, S. A.; Ernsting, N. P. Local THz Time Domain Spectroscopy of Duplex DNA via Fluorescence of an Embedded Probe. *J. Phys. Chem. B* **2009**, *113*, 15619−15628.

DOI: 10.1021/acs.jpclett.5b00653
J. Phys. Chem. Lett. 2015, 6, 1754−1760

(25) Banerjee, D.; Pal, S. K. Dynamics in the DNA Recognition by DAPI: Exploration of the Various Binding Modes. *J. Phys. Chem. B* **2008**, *112*, 1016−1021.
(26) Andreatta, D.; Sen, S.; Pérez Lustres, J. L.; Kovalenko, S. A.; Ernsting, N. P.; Murphy, C. J.; Coleman, R. S.; Berg, M. A. Ultrafast Dynamics in DNA: "Fraying" at the End of the Helix. *J. Am. Chem. Soc.* **2006**, *128*, 6885−6892.
(27) Andreatta, D.; Pérez Lustres, J. L.; Kovalenko, S. A.; Ernsting, N. P.; Murphy, C. J.; Coleman, R. S.; Berg, M. A. Power-Law Solvation Dynamics in DNA over Six Decades in Time. *J. Am. Chem. Soc.* **2005**, *127*, 7270−7271.
(28) Pal, N.; Verma, S. D.; Sen, S. Probe Position Dependent of DNA Dynamics: Comparison of the Time-Resolved Stokes Shift of Groove-Bound to Base-Stacked Probes. *J. Am. Chem. Soc.* **2010**, *132*, 9277−9279.
(29) Verma, S. D.; Pal, N.; Singh, M. K.; Sen, S. Probe Position-Dependent Counterion Dynamics in DNA: Comparison of Time-Resolved Stokes Shift of Groove-Bound to Base-Stacked Probes in the Presence of Different Monovalent Counterions. *J. Phys. Chem. Lett.* **2012**, *3*, 2621−2626.
(30) Sen, S.; Gearheart, L. A.; Rivers, E.; Liu, H.; Coleman, R. S.; Murphy, C. J.; Berg, M. A. Role of Monovalent Counterions in the Ultrafast Dynamics of DNA. *J. Phys. Chem. B* **2006**, *110*, 13248−13255.
(31) Sajadi, M.; Furse, K. E.; Zhang, X.-X.; Dehmel, L.; Kovalenko, S. A.; Corcelli, S. A.; Ernsting, N. P. Detection of DNA-Ligand Binding Oscillations by Stokes-Shift Measurements. *Angew. Chem., Int. Ed.* **2011**, *50*, 9501−9501.
(32) Yang, Y.; Qin, Y.; Ding, Q.; Bakhtina, M.; Wang, L.; Tsai, M.-D.; Zhong, D. Converting a Binding Protein into a Biosensing Conformational Switch Using Protein Fragment Exchange. *Biochemistry* **2014**, *53*, 5505−5514.
(33) Sen, S.; Paraggio, N. A.; Gearheart, L. A.; Connor, E. E.; Issa, A.; Coleman, R. S.; Wilson, D. M., III.; Wyatt, M. D.; Berg, M. A. Effect of Protein Binding on Ultrafast DNA Dynamics: Characterization of a DNA:APE1 Complex. *Biophys. J.* **2005**, *89*, 4129−4138.
(34) Liang, M.; Zhang, X.-X.; Kaintz, A.; Ernsting, N. P.; Maroncelli, M. Solvation Dynamics in a Prototypical Ionic Liquid + Dipolar Aprotic Liquid Mixture: 1-Butyl-3-methylimidazolium Tetrafluoroborate + Acetonotrile. *J. Phys. Chem. B* **2014**, *118*, 1340−1352.
(35) Samanta, A. Solvation Dynamics in Ionic Liquids: What We Have Learned from the Dynamics Fluorescence Stokes Shift Studies. *J. Phys. Chem. Lett.* **2010**, *1*, 1557−1562.
(36) Bhattacharyya, K. Solvation Dynamics and Proton Transfer in Supramolecular Assemblies. *Acc. Chem. Res.* **2003**, *36*, 95−101.
(37) Ghosh, S.; Chattoraj, S.; Bhattacharyya, K. Solvation Dynamics and Intermitten Oscillation of Cell Membrane: Live Chinese Hamster Ovary Cell. *J. Phys. Chem. B* **2014**, *118*, 2949−2956.
(38) Bagchi, B. Anomalous Power Law Decay in Solvation Dynamics of DNA: A Mode Coupling Theory Analysis of Ion Contribution. *Mol. Phys.* **2014**, *112*, 1−9.
(39) Pal, S.; Maiti, P. K.; Bagchi, B.; Hynes, J. T. Multiple Time Scales in Solvation Dynamics of DNA in Aqueous Solution: The Role of Water, Counterions, and Cross-Correlations. *J. Phys. Chem. B* **2006**, *110*, 26396−26402.
(40) Sen, S.; Andreatta, D.; Ponomarev, S. Y.; Beveridge, D. L.; Berg, M. A. Dynamics of Water and Ions Near DNA: Comparison of Simulation to Time-Resolved Stokes-Shift Experiments. *J. Am. Chem. Soc.* **2009**, *131*, 1724−1735.
(41) Furse, K. E.; Corcelli, S. A. The Dynamics of Water at DNA Interfaces; Computational Studies of Hoechst 33258 Bound to DNA. *J. Am. Chem. Soc.* **2008**, *130*, 13103−13109.
(42) Furse, K. E.; Corcelli, S. A. Molecular Dynamics Simulation of DNA Solvation Dynamics. *J. Phys. Chem. Lett.* **2010**, *1*, 1813−1820.
(43) Furse, K. E.; Corcelli, S. A. Dynamical Signature of Abasic Damage in DNA. *J. Am. Chem. Soc.* **2011**, *133*, 720−723.
(44) Halle, B.; Nilsson, L. Does the Dynamic Stokes Shift Report on Slow Protein Hydration Dynamics? *J. Phys. Chem. B* **2009**, *113*, 8210−8213.
(45) Nilsson, L.; Halle, B. Molecular Origin of Time-Dependent Fluorescence Shifts in Proteins. *Proc. Natl. Acad. Sci. U.S.A.* **2005**, *102*, 13867−13872.
(46) Golosov, A. A.; Karplus, M. Probing Polar Solvation Dynamics in Proteins; A Molecular Dynamics Simulation Analysis. *J. Phys. Chem. B* **2007**, *111*, 1482−1490.
(47) Sterpone, F.; Stirnemann, G.; Laage, D. Magnitude and Molecular Origin of Water Slowdown Next to a Protein. *J. Am. Chem. Soc.* **2012**, *134*, 4116−4119.
(48) Pizziutti, F.; Marchi, M.; Sterpone, F.; Rossky, P. J. How Protein Surfaces Induce Anomalous Dynamics of Hydration Water. *J. Phys. Chem. B* **2007**, *111*, 7584−7590.
(49) Bizzarri, A. R.; Cannistraro, S. Molecular Dynamics of Water at the Protein-Solvent Interface. *J. Phys. Chem. B* **2002**, *106*, 6617−6633.
(50) Lagi, M.; Baglioni, P.; Chen, S.-H. Logarithmic Decay in Single-Particle Relaxation of Hydrated Lysozyme Powder. *Phys. Rev. Lett.* **2009**, *103*, 108102.
(51) Kämpf, K.; Klameth, F.; Vogel, M. Power-Law and Logarithmic Relaxations of Hydrated Proteins: A Molecular Dynamics Simulation Study. *J. Chem. Phys.* **2012**, *137*, 205105.
(52) Volk, M.; Kholodenko, Y.; Lu, H. S. M.; Gooding, E. A.; DeGrado, W. F.; Hochstrasser, R. M. Peptide Conformational Dynamics and Vibrational Stark Effects Following Photoinitiated Disulfide Cleavage. *J. Phys. Chem. B* **1997**, *101*, 8607−8616.
(53) Li, T. Validity of Linear Response Theory for Time-Dependent Fluorescence in *Staphylococcus* Nuclease. *J. Phys. Chem. B* **2014**, *118*, 12952−12959.
(54) Case, D. A.; et al.*AMBER 12*; University of California: San Francisco, 2012.
(55) Spackova, N.; Cheatham, T. E., III; Ryjacek, F.; Lankas, F.; Meervelt, L. v.; Hobza, P.; Sponer, J. Molecular Dynamics Simulation and Thermodynamics Analysis of DNA-Drug Complexes. Minor Groove Binding between 4′,6-Diamidino-2-phenylindole and DNA Duplexes in Solution. *J. Am. Chem. Soc.* **2003**, *125*, 1759−1769.
(56) Fennell, C. J.; Gezelter, J. D. Is the Ewald Summation Still Necessary? Pairwise Alternatives to the Accepted Standard for Long-Range Electrostatics. *J. Chem. Phys.* **2006**, *124*, 234104.
(57) Kubo, R. The Fluctuation-Dissipation Theorem. *Rep. Prog. Phys.* **1966**, *29*, 255−284.
(58) Frauenfelder, H.; Sligar, S. G.; Wolynes, P. G. The Energy Landscapes and Motions of Proteins. *Science* **1991**, *254*, 1598−1603.
(59) Metzler, R.; Jeon, J.-H.; Cherstvy, A. G.; Barkai, E. Anomalous Diffusion Models and their Properties: Non-Stationary, Non-Ergodicity, and Ageing at the Centenary of Single Particle Tracking. *Phys. Chem. Chem. Phys.* **2014**, *16*, 24128−24164.
(60) Schulz, J. H. P.; Barkai, E.; Metzler, R. Aging Effects and Population Splitting in Single-Particle Trajectory Averages. *Phys. Rev. Lett.* **2013**, *110*, 020602.
(61) Cherstvy, A. G.; Metzler, R. Population Splitting, Trapping, and Non-Ergodicity in Heterogeneous Diffusion Processes. *Phys. Chem. Chem. Phys.* **2013**, *15*, 20220−20235.
(62) Shin, J.; Cherstvy, A. G.; Metzler, R. Kinetics of Polymer Looping with Macromolecular Crowding: Effects of Volume Fraction and Crowder Size. *Soft Matter* **2015**, *11*, 472−488.
(63) Bel, G.; Barkai, E. Weak Ergodicity Breaking in the Continuous-Time Random Walk. *Phys. Rev. Lett.* **2005**, *94*, 240602.
(64) Laage, D.; Hynes, J. T. A Molecular Jump Mechanism of Water Reorientation. *Science* **2006**, *311*, 832−835.
(65) Yamamoto, E.; Akimoto, T.; Yasui, M.; Yasuoka, K. Origin of Subdiffusion of Water Molecules on Cell Membrane Surfaces. *Sci. Rep.* **2014**, *4*, 4720.

DOI: 10.1021/acs.jpclett.5b00653
J. Phys. Chem. Lett. 2015, 6, 1754−1760